THE JOURNAL OF BIOLOGICAL CHEMISTRY
Vol. 274, No. 39, Issue of September 24, pp. 27448–27456, 1999

Printed in U.S.A.

Kinetic Characterization of a Monomeric Unconventional Myosin V Construct*

(Received for publication, May 24, 1999, and in revised form, July 19, 1999)

Kathleen M. Trybus‡, Elena Krementsova, and Yelena Freyzon§

From the Department of Physiology and Molecular Biophysics, University of Vermont, Burlington, Vermont 05405

An expressed, monomeric murine myosin V construct composed of the motor domain and two calmodulin-binding IQ motifs (MD(2IQ)) was used to assess the regulatory and kinetic properties of this unconventional myosin. In EGTA, the actin-activated ATPase activity of MD(2IQ) was 7.4 ± 1.6 s^{-1} with a K_{app} of ~1 μM (37 °C), and the velocity of actin movement was ~0.3 μm/s (30 °C). Calcium inhibited both of these activities, but the addition of calmodulin restored the values to ~70% of control, indicating that calmodulin dissociation caused inhibition. In contrast to myosin II, MD(2IQ) is highly associated with actin at physiological ionic strength in the presence of ATP, but the motor is in a weakly bound conformation based on the pyrene-actin signal. The rate of dissociation of acto-MD(2IQ) by ATP is fast (>850 s^{-1}), and ATP hydrolysis occurs at ~200 s^{-1}. The affinity of acto-MD(2IQ) for ADP is somewhat higher than that of smooth S1, and ADP dissociates more slowly. Actin does not cause a large increase in the rate of ADP release, nor does the presence of ADP appreciably alter the affinity of MD(2IQ) for actin. These kinetic data suggest that monomeric myosin V is not processive.

Conventional muscle myosin II polymerizes into filaments and is designed to interact with actin as part of an ensemble, and the kinetic properties of myosins isolated from these tissues reflect this role. Their so-called "duty cycle," *i.e.* the length of time the myosin spends in a force- or motion-producing state, is relatively low compared with the overall cycle time determined by the ATPase activity. This feature allows for speed of contraction, and much of the cycle is spent in a state that is dissociated from actin. In contrast, unconventional myosins are nonfilamentous, and most of these classes of myosin will probably operate in much smaller groups or potentially even individually. Because of these different functional roles, the kinetic properties of these motors are expected to be quite different from the well characterized myosin IIs.

Murine myosin V is a member of the class of unconventional myosins that is implicated in organelle movement and membrane trafficking based on a number of cellular and genetic studies. Mutations in murine myosin V result in a range of defects, from impaired pigment granule movement, resulting in a dilute coat color, to a lack of smooth endoplasmic reticulum in the dendritic spines of Purkinje cells, which may be the cause of the neurological defect that results in early postnatal death (reviewed in Ref. 1).

Myosin V is particularly interesting from several points of view. It is a dimeric molecule that has an unusually long neck, three times that of myosin II. This region of the molecule has been proposed to act as a lever arm that ultimately results in relative sliding of actin and myosin. The neck region contains six IQ motifs that have the consensus sequence (IQ*XX*IRG*XXX*R) for binding of calmodulin or myosin light chains. Thus, the potential for calcium-dependent regulation of motor activity also exists for this myosin. Because its cellular role may require it to work alone in the cell, myosin V has also been proposed to be a processive motor that undergoes multiple ATPase cycles before dissociating from its actin track. In addition, the globular tail domain beyond the coiled-coil region is believed to be the cargo-binding domain (reviewed in Ref. 1).

The full-length dimeric myosin V has been isolated from chick brain (2), but the quantities that can be obtained are limited, precluding a detailed characterization of the molecule. The strategy we chose was to express shorter monomeric constructs of murine myosin V using the baculovirus/insect cell expression system. We then used these simpler monomeric molecules to begin our characterization of myosin V, much as proteolytic fragments of conventional myosin II have been used to obtain a wealth of information about these myosins.

Here we show that the MD(2IQ)[1] construct (motor domain and two IQ motifs plus two calmodulins) has the potential to be regulated by calcium but only under conditions where excess calmodulin is not present. Thus, the mechanism of inhibition appears to be dissociation of a bound calmodulin. In addition, transient kinetics were used to measure many of the elementary steps in the acto-MD(2IQ) ATPase cycle. These measurements suggest that the monomeric MD(2IQ) construct is not kinetically processive.

MATERIALS AND METHODS

Design and Purification of Constructs—Three constructs were analyzed here. All were derived from the murine myosin V clone (3) (accession number X57377), which was a generous gift from Nancy Jenkins. The motor domain (MD) ends at Asp^{764}, MD(1IQ) ends at Thr^{795}, and MD(2IQ) ends at Thr^{820}. A dimeric MD(2IQ) construct was made by adding the following sequences after Thr^{820}: a 32-amino acid leucine zipper, followed by a portion of the smooth muscle myosin rod containing the S2.2 epitope. The latter piece of DNA was derived from the "0-heptad zipper" construct described by Trybus *et al.* (4). Flag epitope (DYKDDDDK) was cloned at the C terminus of all heavy chain constructs to facilitate purification.

Recombinant baculovirus encoding for the different heavy chain con-

* This work was supported by National Institutes of Health Grant HL38113 (to K. M. T.). The costs of publication of this article were defrayed in part by the payment of page charges. This article must therefore be hereby marked "*advertisement*" in accordance with 18 U.S.C. Section 1734 solely to indicate this fact.

‡ To whom correspondence should be addressed: Dept. of Physiology and Molecular Biophysics, Given Bldg. E205, University of Vermont, Burlington, VT 05405. Tel.: 802-656-8750; Fax: 802-656-0747; E-mail: trybus@salus.med.uvm.edu.

§ Present address: Whitehead Institute for Biomedical Research, Massachusetts Institute of Technology, Cambridge, MA 02142.

[1] The abbreviations used are: MD(2IQ), myosin V motor domain and two IQ motifs, plus two bound calmodulins; MD(1IQ), myosin V motor domain and one IQ motif with one bound calmodulin; MD, myosin V motor domain; DTT, dithiothreitol; mant, 2′-(or 3′)-*O*-(*N*-methylanthraniloyl).

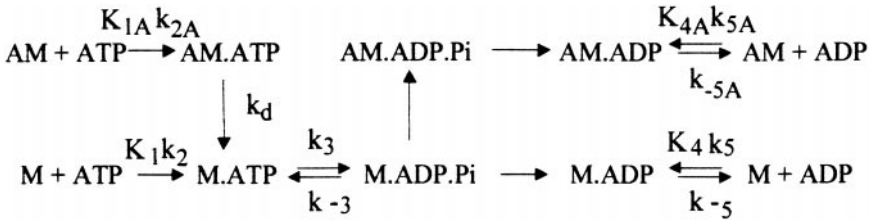

SCHEME 1

structs was isolated by conventional protocols (5). Sf9 cells in suspension culture were infected with recombinant virus coding for the heavy chain and harvested 65–75 h later. For MD(1IQ) and MD(2IQ), there was sufficient endogenous cellular calmodulin to saturate the IQ motifs. Because calmodulin from diverse sources (chicken, rat, and human) is completely conserved at the amino acid level, we were able to infect with only one virus. Recombinant proteins were isolated on an anti-FLAG affinity column (Sigma). Typical yields were 1–1.5 mg of protein/10^9 Sf9 cells (300-ml suspension culture).

Densitometry—Gel images were captured in digital format using a Kodak Digital Science DC120 zoom digital camera, and the band intensity was quantified using the Kodak Digital Science 1D image analysis software package.

Labeling of Actin with Pyrene-Iodoacetamide—Actin (1 mg/ml in 10 mM imidazole, pH 7, 10 mM NaCl, 1 mM $MgCl_2$, 1 mM MgATP) was fully reduced by the addition of 2 mM DTT at pH 8 and then dialyzed overnight into 10 mM imidazole, pH 7.8, 0.1 M KCl, 1 mM $MgCl_2$, 1 mM NaN_3. A 2-fold molar excess of pyrene-iodoacetamide (48 μM) (Molecular Probes, Inc., Eugene, OR) was added from a 4 mM stock in dimethyl formamide. After 20 h of labeling in the dark on ice, the actin was pelleted in the Beckman TL-100 at 350,000 $\times$ *g* for 1 h. The pellet was resuspended in 10 mM HEPES, pH 7, 0.1 M NaCl, 5 mM $MgCl_2$, 1 mM EGTA, 1 mM NaN_3, 1 mM DTT. Protein concentration was determined by Bradford reagent with bovine serum albumin as a standard.

Steady-state ATPase Assays—Actin-activated ATPase assays were performed at 37 °C in 10 mM imidazole, pH 7, 8 mM KCl, 1 mM $MgCl_2$, 1 mM EGTA, 1 mM DTT, 1 mM NaN_3 with or without 1.5 mM $CaCl_2$. One data set was collected in 10 mM HEPES, pH 7, 0.1 M NaCl, 5 mM $MgCl_2$, 1 mM EGTA, 1 mM NaN_3, 1 mM DTT at 20 °C for comparison with the transient kinetic measurements. Inorganic phosphate was determined colorimetrically (6) at six time points per actin concentration, using SDS to stop the reaction.

Motility Assay—The motility assay was performed at 30 °C in 25 mM imidazole, pH 7.5, 25 mM KCl, 4 mM $MgCl_2$, 1 mM EGTA, 0.5% methylcellulose, 1 mM MgATP, 10 mM DTT, 3 mg/ml glucose, 0.1 mg/ml glucose oxidase, 0.018 mg/ml catalase, with or without 1.5 mM $CaCl_2$, essentially as described in Ref. 7. Monoclonal anti-FLAG antibody, or antibody S2.2 (8) in the case of the dimeric MD(2IQ), was used for attachment to the nitocellulose coverslip. For measurements with excess calmodulin, the motility solutions also contained 0.1 mg/ml calmodulin.

Transient Kinetic Experiments—All kinetic experiments were done in 10 mM HEPES, pH 7, 0.1 M NaCl, 5 mM $MgCl_2$, 1 mM EGTA, 1 mM NaN_3, 1 mM DTT at 20 °C using a Kin-Tek stopped flow spectophotometer and a 100-watt mercury lamp. The concentration of MD(2IQ) was 0.5–2 μM, and when appropriate, actin was added at 1.2–1.3 times the MD2(IQ) concentration. For tryptophan fluorescence, the exciting beam was passed through a 294-nm interference filter, and the emission was detected after passing through a 340-nm interference filter. For 90° light scattering, the exciting beam was passed through a 294-nm interference filter, and the emission was detected with a 294-nm interference filter. Mant nucleotides and pyrene actin were excited using a 360-nm interference filter, and emission was detected with a 400-nm cut-off filter. Mant nucleotides (2′ or 3′) were purchased from Molecular Probes. All nucleotide stocks were prepared with an equimolar amount of magnesium. All of the transients shown are the average of three or four independent mixings. The signal averaging and fitting was done using Kin-Tek software. Note that the final concentrations of protein and nucleotide after mixing equal volumes of the two syringes are half the initial values.

Interpretation of Kinetic Data—Single exponential data were fit to the equation $y = c + a_1(\exp{-\lambda_1 t})$, and double exponentials were fit to $y = c + a_1(\exp{-\lambda_1 t}) + a_2(\exp{-\lambda_2 t})$, where c is a constant and a_1 and a_2 are the amplitudes of the signal. The data are interpreted in terms of standard schemes developed from analysis of conventional myosin II (9, 10) In Scheme 1, K_i values are equilibrium association constants (k_{+i}/k_{-i}), and k_{+i} and k_{-i} are rate constants. In Scheme 2, K_A, K_D, K_{AD}, and K_{DA} are equilibrium dissociation constants. $K_{AD} = k_{-5A}/K_{4A}k_{5A}$ and $K_D = k_{-5}/K_4k_5$. In all three schemes, *A* represents actin and *M* represents the MD(2IQ) construct.

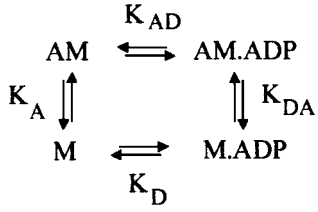

SCHEME 2

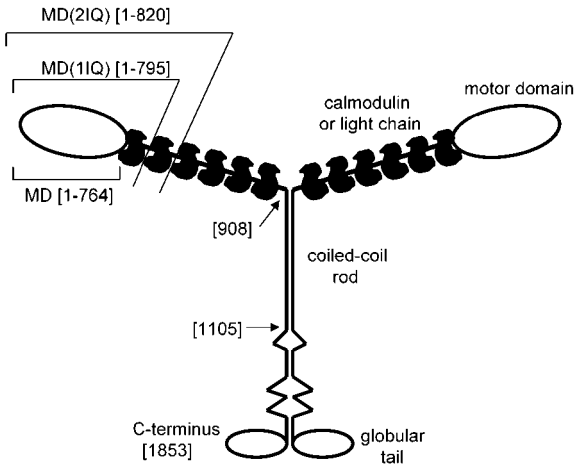

FIG. 1. **Schematic diagram of myosin V.** Shown is a schematic diagram of murine myosin V, adapted from Ref. 2. The molecule is dimeric and nonfilamentous. The three monomeric constructs expressed here are MD, MD(1IQ), and MD(2IQ), followed by the amino acid numbers they contain in *brackets*. Calmodulin molecules are indicated by the *filled black shapes*. The amino acid number at the head/rod junction, at the end of the first coiled-coil rod region, and at the end of the full-length molecule are also indicated in *brackets*.

RESULTS

Description of the Constructs—Three monomeric constructs derived from the murine myosin V clone were expressed in Sf9 cells. MD contains only the catalytic domain (heavy chain residues 1–764). MD(1IQ) contains the motor domain plus one IQ motif for binding of calmodulin (heavy chain residues 1–795), while MD(2IQ) contains the motor domain plus 2IQ motifs (heavy chain residues 1–820) (Fig. 1). The purified MD(1IQ) and MD(2IQ) constructs have bound calmodulin, which shows its characteristic calcium-dependent shift in mobility in SDS-polyacrylamide gel electrophoresis (Fig. 2). The purified constructs show a stoichiometry of calmodulin/heavy chain that is consistent with the number of calmodulin-binding motifs present in the construct, within experimental error (1.3 for MD(1IQ) and 2.2 for MD(2IQ), average slope from five different gel loadings).

Steady-state Activity—The steady-state ATPase activity as a function of actin concentration was assessed for MD, MD(1IQ),

and MD(2IQ) in the presence or absence of calcium (37 °C, 10 mM imidazole, pH 7, 8 mM KCl, 1 mM $MgCl_2$, 1 mM EGTA, 1 mM DTT, 1 mM NaN_3, with or without 1.5 mM $CaCl_2$) to determine if the activity of any of these constructs is regulated by calcium. As expected, calcium had no effect on the activity of MD (V_{max} = 6.3 ± 0.3 s^{-1}, K_{app} = 0.3 ± 0.07 μM) (Fig. 3*A*). MD(1IQ) showed lower activity at subsaturating actin concentrations in the presence of calcium (V_{max} = 8.5 ± 1.5 s^{-1}; K_{app} = 2.7 ± 1.0 μM) compared with that seen in EGTA (V_{max} = 8.7 ± 0.5 s^{-1}; K_{app} = 1.0 ± 0.2 μM), but this was an effect on K_{app} and not on V_{max} (Fig. 3*B*). In contrast, the activity of MD(2IQ) was high in the presence of EGTA (V_{max} = 7.4 ± 0.6 s^{-1}, K_{app} = 1.2 ± 0.3 μM) and inhibited to a value of approximately 1 s^{-1} in the presence of calcium (Fig. 3*C*). In all instances, the motor activity in the absence of actin was <0.1 s^{-1}.

The ATPase values reported here for the monomeric constructs are lower than reported for the native dimeric molecule isolated from tissue (27 s^{-1} in the presence of calcium) (11). Thus, we engineered a double-headed MD(2IQ) construct that was dimerized by virtue of the addition of a leucine zipper, a strategy we have previously used (4). Dimerization of our expressed construct did not increase, and in fact somewhat reduced, the activity in EGTA (V_{max} = 3.2 ± 0.32 s^{-1}; K_{app} = 1.6 ± 0.4 μM). As with the monomeric MD(2IQ) construct, the addition of calcium decreased the activity (0.4 s^{-1}). The addition of calmodulin in the presence of calcium increased the ATPase activity to ~70% of the value in EGTA. Therefore, dimerization *per se* does not cause enhanced activity in calcium.

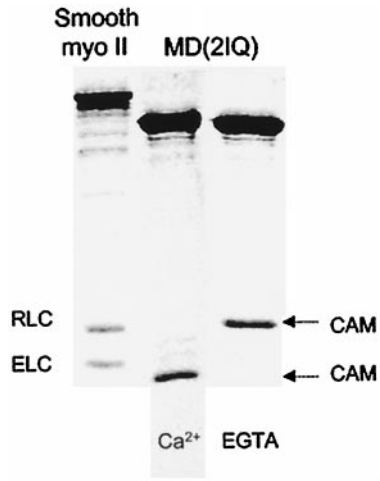

FIG. 2. **Expressed murine myosin V motor domain with two IQ motifs and bound calmodulin.** Shown in an SDS-gel are smooth muscle myosin purified from tissue (*lane 1*) and expressed myosin V motor domain with two IQ motifs and bound calmodulin, MD(2IQ) (*lanes 2* and *3*). Calmodulin undergoes its characteristic calcium-dependent shift in mobility (*lane 2*, calcium; *lane 3*, EGTA). SDS-15% polyacrylamide gel was used.

Rescue of ATPase Activity by Exogenous Calmodulin—Calcium could decrease the enzymatic activity of the MD(2IQ) complex either by changing the conformation of the bound calmodulin or by causing its dissociation from the heavy chain. To discriminate between these two possibilities, 12 μM exogenous calmodulin was added to the ATPase solution. The addition of calmodulin to MD(2IQ) in the presence of calcium resulted in a 10-fold activation of actin-activated ATPase activity (Table I). The simplest explanation of these data is that calmodulin dissociation from site 2 (with site 1 adjacent to the motor domain) causes the calcium-dependent decrease in activity.

Dissociation of some calmodulin from the MD(2IQ) complex in the presence of calcium was also observed by an actin pelleting assay. MD(1IQ) retained all of its bound calmodulin both in the presence and absence of calcium. In contrast, MD(2IQ) released some of its calmodulin into the supernatant in the presence of calcium. Note that the protein concentration used in the pelleting assay is nearly 100-fold greater than that used for the ATPase assays, and thus it is likely that more calmodulin is dissociated during activity measurements.

Motility of Expressed Constructs—The motility of the MD, MD(1IQ), and MD(2IQ) constructs were examined in the presence and absence of calcium (Table II). All three constructs moved actin in the absence of calcium, whether or not exogenous calmodulin was added. There was a trend toward faster movement as the length of the neck region increased. The rate of motility of the dimerized MD(2IQ) was the same as that of the monomeric MD(2IQ).

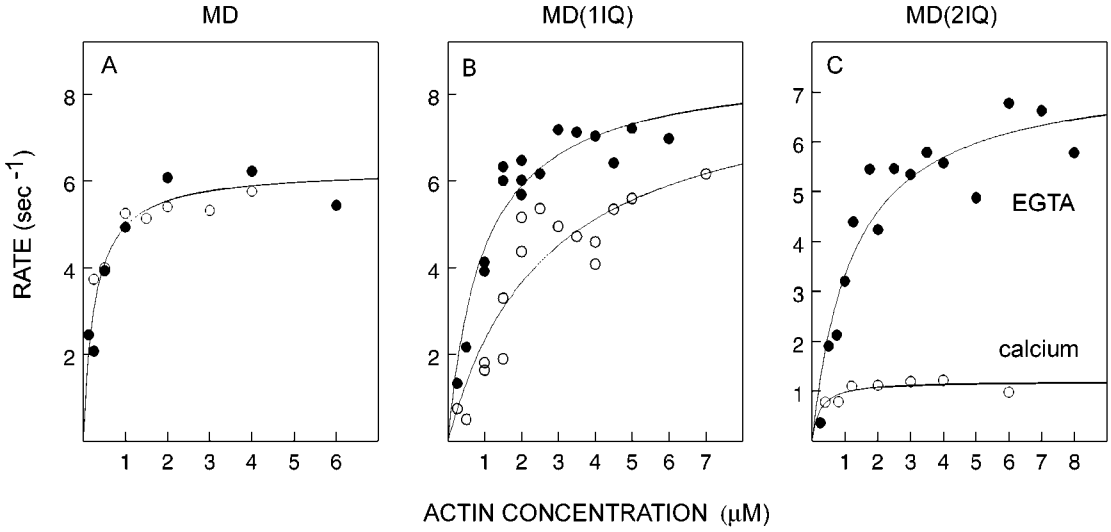

FIG. 3. **The actin-activated ATPase activity of MD(2IQ) is inhibited by calcium.** Steady-state ATPase assays as a function of actin concentration for MD (*A*), MD(1IQ) (*B*), and MD(2IQ) (*C*) in the absence (*filled circles*) or presence (*open circles*) of calcium are shown. MD had a V_{max} = 6.3 ± 0.3 s^{-1} and a K_{app} = 0.3 ± 0.07 μM. MD(1IQ) showed the same V_{max} but a higher K_{app} in the presence of calcium (V_{max} = 8.5 ± 1.5 s^{-1}; K_{app} = 2.7 ± 1.0 μM) compared with that seen in EGTA (V_{max} = 8.7 ± 0.5 s^{-1}; K_{app} = 1.0 ± 0.2 μM). In contrast, the activity of MD(2IQ) was high in the presence of EGTA (V_{max} = 7.4 ± 0.6 s^{-1}; K_{app} = 1.2 ± 0.3 μM) and decreased to ~1 s^{-1} in the presence of calcium. Conditions were as follows: 10 mM imidazole, pH 7, 8 mM KCl, 1 mM $MgCl_2$, 1 mM EGTA, 1 mM DTT, 1 mM NaN_3, with or without 1.5 mM $CaCl_2$ at 37 °C.

Calcium had no effect on the rates of motility for MD and MD(1IQ), consistent with the ATPase measurements, which showed no effect of calcium on V_{max}. Paralleling the inhibition of ATPase activity observed for MD(2IQ) in the presence of calcium, no actin movement was observed under these conditions. The addition of 6 μM calmodulin to the motility solutions restored movement to levels comparable with that observed in EGTA, consistent with the restoration of ATPase activity that occurred upon the addition of exogenous calmodulin.

Degree of Association in the Presence of MgATP—An unusual feature of the myosin V constructs is the high degree of association with actin in the presence of MgATP, even for these monomeric constructs. Both pelleting and light scattering experiments (Fig. 4) show that near physiologic ionic strength, most of the MD(2IQ) is associated with actin in the presence of MgATP. Under the same conditions, smooth or skeletal muscle myosin II would be >90% dissociated from actin.

Rate of ATP Binding to MD(2IQ)—The MD(2IQ) construct was selected for further analysis by transient kinetics. Table III summarizes the values that were obtained. All of these experiments were conducted in 10 mM HEPES, pH 7, 0.1 M NaCl, 5 mM $MgCl_2$, 1 mM EGTA, 1 mM NaN_3, 1 mM DTT at 20 °C for comparison with values previously obtained for conventional muscle myosins (reviewed in Refs. 9 and 10). The maximal steady-state actin-activated ATPase for MD(2IQ) under the above conditions was 3.3 ± 0.9 s^{-1}, with a K_{app} ~20 μM (note that the conditions for Fig. 3 are 8 mM KCl and 37 °C).

The rate of nucleotide binding to MD(2IQ) was followed by the increase in intrinsic tryptophan fluorescence (Fig. 5). At low ATP concentrations, the rate of the transient increased linearly with ATP, defining K_1k_2 (Scheme 1) as 7×10^5 M^{-1} s^{-1}. Fiting the data to a hyperbola gave a a maximum rate of 198 ± 13 s^{-1}, which is likely to be a measure of the rate of the hydrolysis step ($k_3 + k_{-3}$), by analogy with studies on other myosins where the maximum rate of the fluorescence change has been equated with the rate of ATP cleavage determined by quench flow measurements (12). The amplitude of the fluorescence signal decreased from 5% at low ATP concentrations to 3% at high ATP concentrations. This pattern is consistent with a two-step binding scheme, with approximately half of the fluorescence change attributed to binding and the other half to hydrolysis. Binding of ADP caused no change in fluorescence.

The source of the tryptophan(s) that contribute to the change upon nucleotide binding would be expected to be conserved among various myosins. The MD(2IQ) construct has eight tryptophan residues, seven of which are in the catalytic domain. Two of these Trp residues are conserved between smooth, skeletal, *Dictyostelium*, and myosin V; they are equivalent to Trp^{441} and Trp^{512} in the smooth muscle numbering system. The varying amplitude of the signal enhancement seen with different myosins may reflect variable contributions of the nonconserved Trp residues to the base-line signal, since their level of fluorescence is dependent on their environment.

Mant Nucleotide Binding to MD(2IQ) and Acto-MD(2IQ)—Fluorescent nucleotides have proved to be a useful way of determining the rate of nucleotide binding to myosins, particularly when the intrinsic tryptophan signal is small or nonexistent. Similar to other myosins, nucleotide binding to MD(2IQ) caused an increase in mant fluorescence. The rate of mant-ATP binding to MD(2IQ) was similar to that determined for ATP, with an apparent second order rate constant of 7×10^5 M^{-1} s^{-1} (Fig. 6*C*, *open circles*). The use of the fluorescent nucleotide also allowed the value for mant-ADP binding to be determined, for which there was no corresponding intrinsic tryptophan signal. The signal was biphasic, with the rate as a function of nucleotide concentration defining apparent second order rate constants of 4×10^6 M^{-1} s^{-1} and 4×10^5 M^{-1} s^{-1} (Fig. 6*A*, *open circles*).

The rate of mant-ADP and mant-ATP binding to acto-MD(2IQ) was also determined (Fig. 6, *A* and *C*, *filled circles*). Binding of mant-ATP fit a single exponential signal (Fig. 6*D*), while binding of mant-ADP was best fit by two exponentials (Fig. 6*B*). The values that were obtained were very similar to those obtained in the absence of actin, implying that actin has little effect on the rate at which nucleotide binds.

Rate of ADP Release from MD(2IQ)—Because ATP but not ADP binding caused a change in tryptophan fluorescence, this signal could be used to determine the rate of ADP release from MD(2IQ). 1 μM MD(2IQ) with varying ADP concentration (4–14 μM) was mixed with 400 μM ATP. The single exponential rise in fluorescence that was observed occurred at a rate of approximately 8–12 s^{-1}, much lower than the ~100 s^{-1} determined at this ATP concentration in the absence of ADP (Fig. 7*A*). Thus, ADP dissociates from MD(2IQ) at approximately 10 s^{-1} (k_{-5}).

The rate of mant-ADP release from MD(2IQ), determined by mixing MD(2IQ) and 14 μM mant-ADP with 1 mM ATP, was 0.6

TABLE I
Restoration of actin-activated ATPase activity by the addition of calmodulin

Conditions were as follows: 10 mM imidazole, pH 7, 8 mM KCl, 1 mM $MgCl_2$, 1 mM EGTA, 1 mM DTT, 1 mM NaN_3, 4 μM actin, with or without 1.5 mM $CaCl_2$, with or without 12 μM calmodulin, 37 °C.

	EGTA	EGTA + calmodulin	Calcium	Calcium + calmodulin
			s^{-1}	
MD(1IQ)	4.1	5.1	3.4	4.1
MD(2IQ)	5.1	5.9	0.4	4.3

TABLE II
Motility of expressed constructs

Numbers in parentheses indicate number of filaments. A minimum of two independent preparations was used for each construct. Conditions were as follows: 10 mM imidazole, pH 7.5, 25 mM KCl, 4 mM $MgCl_2$, 1 mM EGTA, 1 mM NaN_3, with or without 1.5 mM $CaCl_2$, with or without 6 μM calmodulin, 30 °C.

	EGTA	EGTA + calmodulin	Calcium	Calcium + calmodulin
			$\mu m/s$	
MD	0.099 ± 0.08 (62)		0.074 ± 0.03 (13)	
MD(1IQ)	0.22 ± 0.04 (68)	0.30 ± 0.04 (17)	0.19 ± 0.04 (22)	0.25 ± 0.05 (15)
MD(2IQ)	0.31 ± 0.07 (87)	0.25 ± 0.06 (36)	No movement	0.19 ± 0.05 (12)
MD(2IQ) dimer[a]	0.33 ± 0.03 (24)	0.32 ± 0.03 (18)	ND[b]	ND
	0.31 ± 0.04 (24)[c]	0.23 ± 0.04 (11)[c]		

[a] The MD(2IQ) construct was dimerized by the addition of a leucine zipper. This construct also contained the S2.2 epitope (see "Materials and Methods" for details).
[b] ND, not determined.
[c] Antibody S2.2 was used for attachment to the nitrocellulose coverslip. All other values were obtained using anti-FLAG antibody for attachment to the nitrocellulose coverslip.

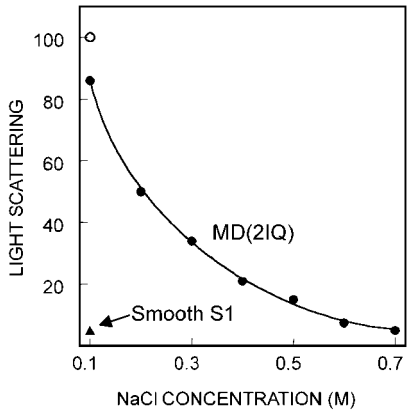

FIG. 4. **MD(2IQ) in the presence of MgATP shows a high degree of association with actin at physiologic ionic strength.** The degree of association of MD(2IQ) with actin was determined by 90° light scattering at 295 nm. The value in the absence of MgATP (*open circle*) was assigned as 100% association as determined by actin pelleting assays. 1 mM MgATP was then added (*filled circles*), followed by further additions of NaCl. The *filled triangle* shows that smooth muscle S1 at 0.1 M NaCl, 1 mM MgATP would be completely dissociated. Conditions were as follows: 1 μM actin, 1 μM MD(2IQ), 10 mM HEPES, pH 7, varying NaCl, 5 mM $MgCl_2$, 1 mM EGTA, 1 mM NaN_3, 1 mM MgATP at 20 °C.

TABLE III
Summary of rate constants (see Scheme 1)

Conditions are as follows: 10 mM HEPES, pH 7, 0.1 M NaCl, 5 mM $MgCl_2$, 1 mM EGTA, 1 mM NaN_3, 1 mM DTT at 20 °C.

Constant	Nucleotide	Value	Nucleotide	Value
K_1k_2	ATP	7×10^5 M^{-1} s^{-1}	Mant-ATP	7×10^5 M^{-1} s^{-1}
$K_{1A}k_{2A}$	ATP	7×10^5 M^{-1} s^{-1}	Mant-ATP	6×10^5 M^{-1} s^{-1}
k_d	ATP	850 s^{-1}		
$k_3 + k_3$	ATP	200 s^{-1}		
K_4k_5			Mant-ADP	4×10^6 M^{-1} s^{-1}, 4×10^5 M^{-1} s^{-1}
$K_{4A}k_{5A}$			Mant-ADP	4×10^6 M^{-1} s^{-1}, 4×10^5 M^{-1} s^{-1}
k_{-5}	ADP	8–12 s^{-1}	Mant-ADP	0.6 s^{-1}
k_{-5A}	ADP	13–22 s^{-1}	Mant-ADP	17–19 s^{-1}

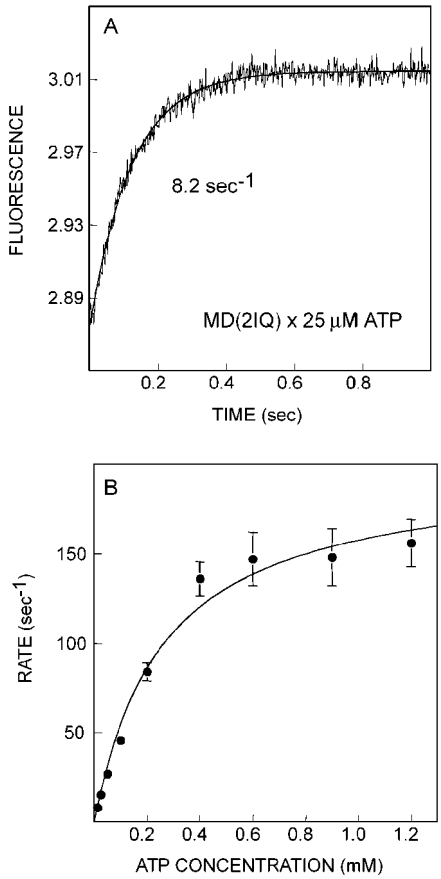

FIG. 5. **Rate of ATP hydrolysis as determined by intrinsic tryptophan fluorescence.** *A*, 2 μM MD(IQ) was mixed with MgATP, and the increase in tryptophan fluorescence as a function of time (*jagged trace*) was fitted to a single exponential (*smooth line*). Note that the concentration of ATP following mixing is half the initial value. *B*, these rates are plotted as a function of ATP concentration. The initial slope defines $K_1k_2 = 7 \times 10^5$ M^{-1} s^{-1}. Fitting the data to a hyperbola gave a maximum rate of 198 ± 13 s^{-1}. Conditions were as follows: 10 mM HEPES, pH 7, 0.1 M NaCl, 5 mM $MgCl_2$, 1 mM EGTA, 1 mM NaN_3, 1 mM DTT at 20 °C.

s^{-1}, an order of magnitude slower than observed for ADP. The dissociation constant of mant-ADP for MD(2IQ), estimated from the ratio of off to on rate constants is ~0.2 μM (0.6 s^{-1}/4 × 10^6 M^{-1} s^{-1}). If the rate of binding of ADP and mant-ADP to MD(2IQ) is similar, mant-ADP would bind tighter to MD(2IQ) than ADP does because of a reduced rate of nucleotide release. A 10-fold tighter binding of mant-ADP compared with ADP was observed with both smooth and skeletal S1 (13).

Rate of Dissociation of Acto-MD(2IQ) by ATP—Light scattering was used to determine the rate of dissociation of acto-MD(2IQ) by ATP (Fig. 8). One μM acto-MD(2IQ) was mixed with increasing concentrations of ATP. The apparent second order rate constant for binding ($K_{1A}k_{2A}$) was 7×10^5 M^{-1} s^{-1}. There was little deviation from a straight line until quite high ATP concentrations, but the extrapolated value estimated from a fit to a hyperbola was approximately 850 s^{-1}. This value could be an underestimate of the maximum rate of dissociation (k_d).

Rate of ADP Release from Acto-MD(2IQ)—Three different signals were used for measuring the rate of ADP release from acto-MD(2IQ). The first method, which used pyrene-labeled actin, also allowed one to determine the affinity of ADP for acto-MD(2IQ). The fluorescence of pyrene-labeled actin is quenched when it is tightly bound to the motor domain. Binding of ATP causes an increase in fluorescence, while binding of ADP causes no change in fluorescence (Fig. 9*A*). When the MD(2IQ)·ADP complex (0–16 μM ADP) is mixed with 1 mM MgATP, the increase in fluorescence is biphasic (Fig. 9*A*), with the amplitude of the fast phase decreasing and the amplitude of the slow phase increasing with ADP concentration (Fig. 9*B*). The fast phase is due to binding of ATP to pyrene-acto-MD(2IQ) that has no ADP bound, while the slow phase is due to binding of ATP to pyrene-acto-MD(2IQ) that has ADP bound. The amplitude dependence of the signal fitted a hyperbola with a midpoint ~2 μM, reflecting the affinity of acto-MD(2IQ) for ADP (K_{AD}). The rate of the slow phase, either when the transient was fitted to two exponentials or at higher ADP when the transient was fitted to a single exponential, was between 13.5 and 14.5 s^{-1}, which is the rate of ADP release from acto-MD(2IQ) (k_{-5A}).

Light scattering was the second method used to measure the rate of ADP release. The acto-MD(2IQ)·ADP complex was mixed with ATP. The ADP concentration was 5–60 μM, severalfold higher than the dissociation constant, and the ATP concentration was 1 mM, so that the rate at which it binds to and dissociates the acto-MD(2IQ) complex is fast compared with the rate of ADP release. The light scattering decrease occurred at a rate of approximately 17–22 s^{-1} (k_{-5A}) (Fig. 7*B*), compared with greater than 200 s^{-1} in the absence of ADP at this ATP concentration. This value also defines the rate at which ADP dissociates from acto-MD(2IQ) (k_{-5A}).

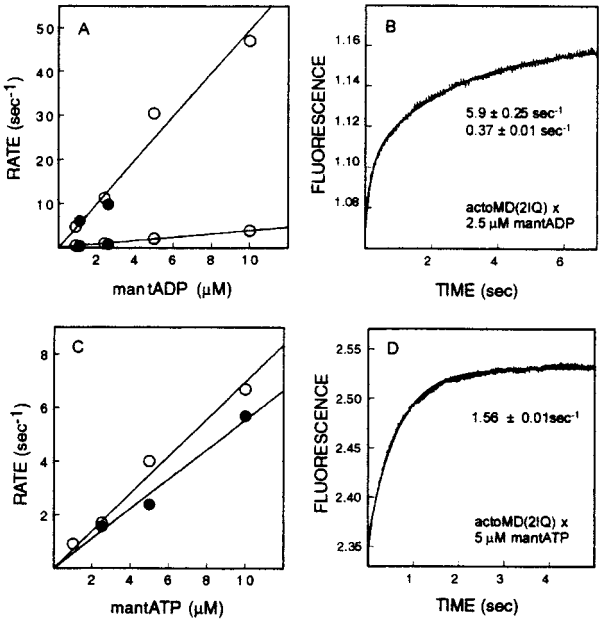

FIG. 6. **Rate of mant-ADP and mant-ATP binding to MD(2IQ) and acto-MD(2IQ).** The rate of mant-ADP (*A*) or mant-ATP binding (*C*) to MD(2IQ) (*open circles*) or acto-MD(2IQ) (*filled circles*) as a function of nucleotide concentration is shown. *B* and *D*, the observed fluorescence increase when mant nucleotides bind to acto-MD(2IQ). Fits are shown by the *smooth line* through the experimental trace (*jagged line*). The rates were biphasic for mant-ADP binding and single exponentials for mant-ATP binding. The apparent second order rate constant for binding to MD(2IQ) is 4×10^6 M^{-1} s^{-1} and 4×10^5 M^{-1} s^{-1} for mant-ADP and 7×10^5 M^{-1} s^{-1} for mant-ATP. Actin had little effect on these values. Conditions were as follows: 10 mM HEPES, pH 7, 0.1 M NaCl, 5 mM $MgCl_2$, 1 mM EGTA, 1 mM NaN_3, 1 mM DTT at 20 °C.

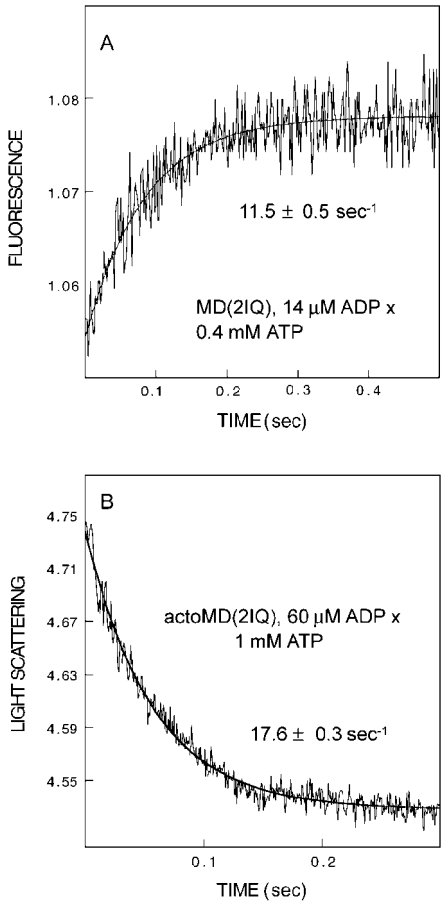

FIG. 7. **Rate of ADP release from MD(2IQ) and acto-MD(2IQ).** *A*, 2 μM MD(2IQ), 14 μM ADP was mixed with 400 μM MgATP, and the increase in intrinsic tryptophan fluorescence as a function of time (*jagged line*) was fitted to a single exponential (*smooth line*). *B*, 0.7 μM acto-MD(2IQ), 60 μM ADP was mixed with 1 mM MgATP, and the decrease in light scattering as a function of time (*jagged line*) was fitted to a single exponential (*smooth line*).

The above experiment was repeated with mant-ADP bound to acto-MD(2IQ). The signal was the decrease in mant fluorescence as the fluorescent nucleotide dissociated from the active site and was replaced with nonfluorescent ATP. The rate of the fluorescence decrease was in the range of 17–19 s^{-1}, in good agreement with the value obtained by light scattering. Thus, ADP and mant-ADP have similar rates of dissociation from acto-MD(2IQ), in contrast to the different rates of dissociation they have from MD(2IQ). This pattern of behavior was also observed for smooth and skeletal S1 (13).

An apparent second order rate constant of $6–11 \times 10^6$ M^{-1} s^{-1} for ADP binding to acto-MD(2IQ) is predicted from a dissociation constant of 2 μM and an off rate of 13–22 s^{-1} (13–22 s^{-1}/2 μM).

Effect of ADP on the Affinity of Actin for MD(2IQ)—The equilibrium dissociation constant of actin for MD(2IQ) and for MD(2IQ)·ADP was determined in the stopped flow (K_A and K_{DA} in Scheme 2). Phalloidin-stabilized pyrene-actin (30 nM) was incubated with varying concentrations of MD(2IQ) or MD(2IQ)·50 μM ADP. The complex was then dissociated by mixing with 10 μM ATP in the stopped flow. The final voltage of the fluorescence signal is constant, since it reflects the fluorescence of 30 nM unbound actin. The initial voltage of the signal decreased as the MD(2IQ) concentration increased, consistent with a higher degree of quenching as more motor binds to the pyrene-actin (14). The amplitudes of the signals, plotted as a function of MD(2IQ) concentration, were fitted to a hyperbola. The dissociation constant was 61 ± 19 nM in the presence of ADP, and 43 ± 12 nM in the absence of ADP (Fig. 10*A*, Table IV).

The rate at which MD(2IQ) (with or without 50 μM ADP) binds to actin was determined by light scattering. The rate decreased from 4.8×10^6 M^{-1} s^{-1} to 3.0×10^6 M^{-1} s^{-1} in the presence of ADP (Fig. 10*B*), showing that the presence of ADP slowed the binding to actin less than 2-fold.

DISCUSSION

Calcium-dependent Regulation of Myosin V's Motor Activity

Studies on tissue-purified myosin V showed that the motility and ATPase activity of this molecule is regulated by calcium (2). To gain insight into the mechanistic basis for this calcium-dependent regulation, we first established the minimal motor whose activity is regulated by calcium. Such an approach with smooth muscle myosin showed that the minimal molecule that is regulated by phosphorylation has two heads and a 15-nm tail, suggesting that both head-head and head-rod interactions are necessary to obtain the "off" state (4). In the case of myosin V, the motility and V_{max} of MD(1IQ) were independent of calcium, but the activity and motility of the monomeric MD(2IQ) construct were substantially inhibited by calcium. Calcium could exert its effect on activity either by altering the conformation of bound calmodulin (like phosphorylation affects the activity of the smooth muscle regulatory light chain) or by dissociation of calmodulin from the heavy chain. Since the addition of exogenous calmodulin rescued the activity of MD(2IQ) to 70% of the activity obtained in EGTA, dissociation appears to be the mechanism for inhibition of actin-activated

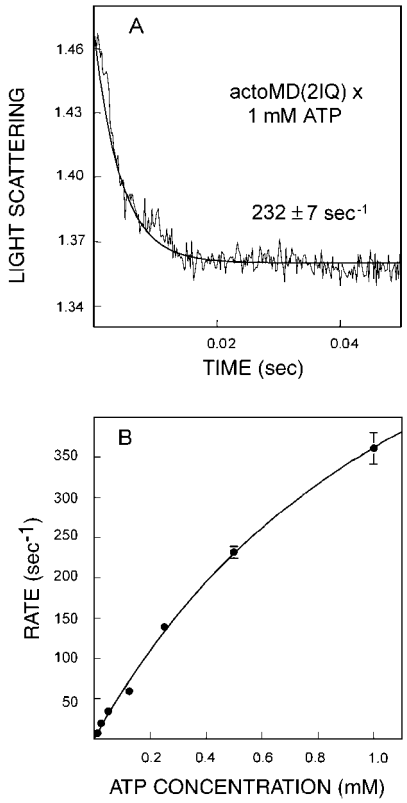

FIG. 8. **ATP rapidly dissociates acto-MD(2IQ).** *A*, 0.7 μM acto-MD(2IQ) was mixed with MgATP, and the decrease in light scattering as a function of time (*jagged line*) was fitted to a single exponential (*smooth line*). Note that the concentration of ATP following mixing is half the initial value. *B*, the rates are plotted as a function of ATP concentration. The apparent second order rate constant for binding ($K_{1A}k_{2A}$) was 7×10^5 M^{-1} s^{-1}, and the extrapolated maximum value estimated from a fit to a hyperbola was ~850 s^{-1}. Conditions were as follows: 10 mM HEPES, pH 7, 0.1 M NaCl, 5 mM $MgCl_2$, 1 mM EGTA, 1 mM NaN_3, 1 mM DTT at 20 °C.

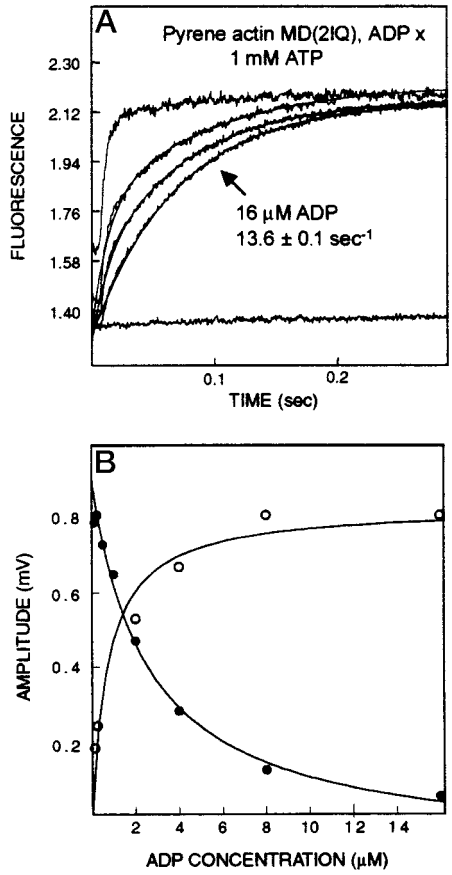

FIG. 9. **Affinity of ADP for acto-MD(2IQ) and its rate of dissociation determined with pyrene-actin.** *A*, 0.5 μM acto-MD(2IQ) and 0, 4, 8, or 16 μM MgADP was mixed with 1 mM MgATP, and the increase in pyrene fluorescence as a function of time (*jagged line*) was fitted to two exponentials, which vary in relative amplitude as the ADP concentration is increased. The *flat trace* was produced by mixing pyrene-labeled actin MD(2IQ) with ADP to show that ADP alone did not dissociate the complex. *B*, the amplitudes of the slow and fast phases are plotted as a function of ADP concentration. The fit to a hyperbola defines an affinity of ADP for acto-MD(2IQ) as ~2 μM. Conditions were as follows: 10 mM HEPES, pH 7, 0.1 M NaCl, 5 mM $MgCl_2$, 1 mM EGTA, 1 mM NaN_3, 1 mM DTT at 20 °C.

ATPase activity. The simplest interpretation of these data is that calmodulin dissociates from site 2 (the second site away from the motor domain). This interpretation assumes that the properties of site 1 are the same in MD(1IQ) as in MD(2IQ), but it is possible that interactions between calmodulins on adjacent sites modulate the properties of the individual sites.

Comparison with Myosin V Isolated from Tissue

Our results differ from those obtained with dimeric chick myosin V isolated from tissue, which showed an actin-activated ATPase activity of 2 s^{-1} in EGTA and 27 s^{-1} in calcium with excess calmodulin (37 °C) (11). Our ATPase values in calcium were never an order of magnitude higher than the rates obtained in EGTA, even with excess calmodulin. A dimerized MD(2IQ) construct also did not show a higher ATPase activity in calcium plus calmodulin than in EGTA.

With regard to motility, calcium stopped movement of both the expressed MD(2IQ) and the tissue-isolated chick myosin V, provided that excess calmodulin was not present (2). In both cases, the addition of calmodulin partially or wholly restored motility to the level seen in EGTA. Paradoxically, activity and motility are therefore uncoupled in the case of the tissue-isolated chick myosin V (high activity and low motility in calcium; low activity but high motility in EGTA), while they are coupled for MD(2IQ) (low activity and low motility in calcium; high activity and high motility in EGTA). Brush border myosin I, a single-headed motor with three IQ motifs, showed a pattern

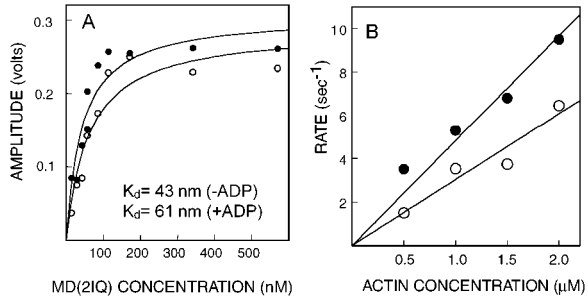

FIG. 10. **Affinity of MD(2IQ) for actin in the presence or absence of ADP.** *A*, phalloidin-stabilized, pyrene-labeled actin (30 nM) plus varying concentrations of MD(2IQ) was mixed with 10 μM MgATP. The amplitude of the signal increases with increasing MD(2IQ) concentration. Half-maximal saturation was obtained at 43 nM. The same experiment was performed, but the acto-MD(2IQ) complex also contained 50 μM ADP. Half-maximal saturation was obtained at 61 nM. These values define the dissociation constant of actin from acto-MD(2IQ) or from acto-MD(2IQ)·ADP. *B*, the rate of association of actin with 0.25 μM MD(2IQ) in the absence (*filled circles*) or presence (*open circles*) of 50 μM ADP was measured by light scattering. Conditions were as follows: 10 mM HEPES, pH 7, 0.1 M NaCl, 5 mM $MgCl_2$, 1 mM EGTA, 1 mM NaN_3, 1 mM DTT at 20 °C.

TABLE IV
Comparison of the interaction of different myosins with ADP (see Scheme 2)

	Myosin V MD(2IQ)[a]	Smooth S1[b]	Skeletal S1[c]
Relative affinity of A for M versus M · ADP (K_{DA}/K_A)	1.4	4–7	30–60
K_{AD}	2 μM	5 μM	120 μM
K_D	(1.4 μM)[d]	1.2 μM	2 μM
K_A	43 nM	3.5 nM	33 nM
K_{DA}	61 nM	24 nM	1 μM
Acceleration of ADP release by actin	2-fold (8–12 to 13–22 s^{-1})	10-fold (2 to 20 s^{-1})	250-fold (2 to >500 s^{-1})

[a] This work.
[b] Ref. 13.
[c] Ref. 29.
[d] Calculated.

of activity similar to that observed with the expressed MD(2IQ). In the presence of calcium, ATPase activity decreased 5-fold and motility ceased, but exogenous calmodulin restored both of these activities (15).

It is striking that the rate of motility (~0.3 μm/s at 24 °C) supported by the full-length construct (2) is similar to that of the expressed MD(2IQ) (~0.3 μm/s at 30 °C). These results raise the possibility that the entire lever arm may not be functioning as a rigid lever that would allow faster motility. Alternatively, the longer necked constructs may have a correspondingly higher dwell time on actin, in which case a potentially longer unitary step size would be balanced by a longer time spent attached to actin (velocity = step size/dwell time).

Is the Activity of the Myosin V Motor Regulated by Calcium in Vivo?

Mutants of Myo2p, a member of the class V myosins in yeast, provide some insights into the potential of this motor to be regulated by calcium. Perhaps most strikingly, a yeast strain that contained a mutant myosin in which the 6IQ motifs were deleted was still able to support growth at 90% that of the wild-type strain (16). Since Myo2p is essential for growth, this result suggests that a motor that lacks the potential to be regulated by calcium via calmodulin binding to the neck still functions well. Furthermore, inactivation of the calcium-binding sites of calmodulin has little effect on the yeast strains carrying this mutation (17). Both of these studies imply that calcium-dependent regulation of myosin V's activity is not essential for proper functioning of myosin V in the cell.

An alternative mechanism for regulation of myosin V's activity is that proteins or lipids on the surface of the cargo vesicle affect myosin V's activity via the tail domain. The potential for this to occur was suggested by studies in which myosin V was isolated bound to its associated vesicles. Only after treatment with a dilute detergent was motility observed, suggesting that inhibitory factors were present on the vesicles (18).

Transient Kinetic Studies of MD(2IQ)

Common Features—The kinetics of several steps in the ATPase cycle of myosin V do not differ significantly from that seen with other myosins (Table III). The rate of dissociation of acto-MD(2IQ) by ATP is fast and extrapolates to approximately 850 s^{-1}, and the rate of ATP hydrolysis is approximately 200 s^{-1}. Thus, like other myosins, myosin V will first dissociate from actin and then hydrolyze ATP. Second order rate constants for nucleotide binding lie within the range of previously established values. The rate of ADP release from acto-MD(2IQ) is fairly slow, between 13 and 22 s^{-1}, but this value is still faster than the maximal velocity from steady-state ATPase measurements (V_{max} = 3.3 ± 0.9 s^{-1} at 0.1 M NaCl and 20 °C) and is therefore not the rate-limiting step in the cycle. The affinity of ADP for acto-MD(2IQ) is high but close to that observed with smooth muscle S1 (13) or brush border myosin I (19) (Table IV).

Unique Features—Myosin V MD(2IQ) differs in several significant ways from smooth and skeletal S1, particularly in the coupling between actin and nucleotide binding (Tables III and IV). Actin accelerates the rate of ADP release from MD(2IQ) by only 2-fold, compared with a 10-fold increase with smooth S1 and a 250-fold increase with skeletal S1 (Table IV). In addition, the presence of ADP does not appreciably alter the affinity of MD(2IQ) for actin or its rate of binding to actin (Fig. 10). In contrast, MgADP weakens the affinity of skeletal S1 for actin to a large extent (~50-fold), and the affinity of smooth S1 for actin by ~4-fold. By calculation, one can also infer that the affinity of ADP for MD(2IQ) and acto-MD(2IQ) is similar and strong (1–2 μM). In the case of smooth and skeletal S1, the tighter binding of ADP for the actin-free motor drives the dissociation of acto-S1 by nucleotides.

Additional evidence that the interaction of myosin V with actin differs from that seen with conventional myosins comes from the use of mant nucleotides and pyrene actin. The signals from these probes have been interpreted in terms of a three-state model, in which actin first forms a collision complex with the motor and then forms an attached state (A-state; nucleotide tightly bound, actin weakly bound), followed by a rotated or rigor-like state (R-state; nucleotide weakly bound, actin tightly bound) (20, 21). The fluorescence of pyrene-labeled actin is high when free or in the A-state (A*) and quenched in the R-state when the motor is tightly bound. Mant nucleotides also distinguish between these two attached states, but in this case the fluorescence is high when the nucleotide is tightly bound to the motor or in the A-state (mant-ADP*) and low when unbound or in the R-state (Scheme 3).

$$\underset{\text{A-state}}{A^* + M \cdot \text{mant-ADP}^*} \leftrightarrow \underset{\text{R-state}}{A^*\text{-}M \cdot \text{mant-ADP}^*} \leftrightarrow \underset{\text{R-state}}{A \cdot M\text{-mant-ADP}} \leftrightarrow A \cdot M + \text{mant-ADP}$$

SCHEME 3

With myosin V, the fluorescence of mant-ADP increases upon binding to acto-MD(2IQ), indicating that nucleotide is tightly bound (Fig. 6). In the ternary complex of pyrene actin-MD(2IQ)·ADP, the pyrene signal is also quenched, showing that actin is tightly bound (Fig. 9). This is unusual in that it implies that both actin and nucleotide are tightly bound to the motor. In contrast, the addition of mant-ADP to smooth muscle acto-S1 did not cause an increase in mant fluorescence, although pyrene fluorescence was quenched in the ternary complex with ADP (13), indicating that the smooth acto-S1·ADP complex was in the "R-state" (tight actin binding, weak nucleotide binding).

Another unique feature of myosin V is that it shows a high degree of association with actin in the presence of MgATP at physiological ionic strength, as determined by light scattering and actin pelleting assays. This was previously observed with the full-length dimeric molecule isolated from tissue (11). Here we show that the high degree of association is a property of the

monomer and does not require the presence of both heads. In contrast, smooth or skeletal S1 would be predominantly dissociated from actin under these conditions. Although light scattering and pelleting assays show a high degree of association, it is interesting to note that the pyrene actin signal is not quenched under these conditions (Fig. 9). This implies that the actin is not tightly bound to the motor and is in the so-called weakly bound "A-state." One region of myosin V that could contribute to a higher degree of association with actin in the presence of ATP is the 50/20-kDa loop, which is thought to be involved in the initial electrostatic interaction of myosin and actin. Although the sequence of this loop varies even among myosin IIs, there are approximately a dozen more amino acids in this region of yeast, mouse, and chicken myosin V that are not found in other myosins. It is possible that this additional sequence could act as a tether to produce the observed high degree of association in the steady state.

Is Myosin V Processive?

This study also addresses the question of whether a monomeric construct of myosin V is kinetically processive. Criteria for kinetic processivity, which is defined as the average number of ATPase cycles before dissociation of the actin-motor complex, were established from recent studies with the microtubule-based motors kinesin and non-claret disjunctional protein (NCD), and these will be applied to MD(2IQ) (22–24).

The first criterion is the ratio of V_{max} to the rate constant of dissociation of the motor by ATP. A value <1 indicates low processivity. At 20 °C and 0.1 M NaCl, the steady-state ATPase activity of MD(2IQ) is 3.3 s^{-1}, and the rate of dissociation is approximately 850 s^{-1}, yielding a value of 0.004, which implies that monomeric myosin V is not processive. In other words, because of the fast rate of dissociation, MD(2IQ) is more likely to dissociate from actin than to undergo another ATPase cycle without dissociation. For comparison, the value obtained with kinesin monomer is 0.75 (60 s^{-1}/80 s^{-1}), and the value for kinesin dimer is >2 (26 s^{-1}/12 s^{-1}) (22, 23, 25, 26). The interpretation of these data was that the kinesin monomer showed a small degree of processivity, while the dimer was quite processive. The kinesin dimer has also been shown to be mechanically processive (27, 28).

A second criterion was the second order rate constant derived from $k_{cat}/K_{app.}$ A value of $>10^7$ M^{-1} s^{-1} indicates many ATPase cycles per encounter. The processive kinesin dimer gave a value of 1.5×10^8 M^{-1} s^{-1} (38 s^{-1}/0.25 μM) (25). MD(2IQ) was 1.7×10^5 M^{-1} s^{-1} at 20 °C and 0.1 M NaCl (3.3 s^{-1}/20 μM) and 7.4×10^6 M^{-1} s^{-1} at 8 mM NaCl and 37 °C (7.4 s^{-1}/1 μM), both values indicating a nonprocessive motor.

The last criteria was the ratio of the rate of motility/V_{max}. The smaller this ratio, the higher the duty cycle and therefore the larger the degree of processivity. This is because the rate of motility is inversely proportional to the time attached to actin. The closer the attached time comes to the total cycle time, the smaller the ratio of motility/V_{max} becomes. For MD(2IQ), the ratio is 0.04 (0.3 μm/s/7.4 s^{-1}), which is lower than smooth or skeletal S1, but not as low as obtained for the processive kinesin dimer (0.015).

In summary, the kinetic evidence does not support the idea that the myosin V monomer is processive. These data do not exclude the possibility that the two-headed myosin V species is processive, and we are currently extending our kinetic studies to dimeric myosin V. Changes in several rate constants would enhance the chance that the dimeric species could be processive. These would include increasing the duty cycle by decreasing the ADP release rate or decreasing the rate of dissociation of acto-MD(2IQ) by ATP. *A priori*, there is no reason to assume that myosin V must be a processive motor. An equally plausible alternative mechanism would be that several myosin V molecules work in concert to move an organelle along an actin track without it diffusing away from its track. The architecture of myosin V, with its long neck region, may enhance the chance that the second head finds a new actin binding site before the first head dissociates. However, this sort of mechanism would be quite different from the coordinated head action of the processive motor kinesin, in which the heads are closely coupled and not interrupted by a light chain-binding neck region.

Acknowledgments—We thank Mike Geeves and Susan Lowey for critically reading this manuscript and for helpful comments.

REFERENCES

1. Mermall, V., Post, P. L., and Mooseker, M. S. (1998) *Science* **279,** 527–533
2. Cheney, R. E., O'Shea, M. K., Heuser, J. E., Coelho, M. V., Wolenski, J. S., Espreafico, E. M., Forscher, P., Larson, R. E., and Mooseker, M. S. (1993) *Cell* **75,** 13–23
3. Mercer, J. A., Seperack, P. K., Strobel, M. C., Copeland, N. G., and Jenkins, N. A. (1991) *Nature* **349,** 709–713
4. Trybus, K. M., Freyzon, Y., Faust, L. Z., and Sweeney, H. L. (1997) *Proc. Natl. Acad. Sci. U. S. A.* **94,** 48–52
5. O'Reilly, D. R., and Miller, L. K. L. V. A. (1992) *Baculovirus Expression Vectors: A Laboratory Manual*, W. H. Freeman, New York
6. White, H. D. (1982) *Methods Enzymol.* **85,** 698–708
7. Warshaw, D. M., Desrosiers, J. M., Work, S. S., and Trybus, K. M. (1990) *J. Cell Biol.* **111,** 453–463
8. Trybus, K. M., and Henry, L. (1989) *J. Cell Biol.* **109,** 2879–2886
9. Taylor, E. W. (1979) *Crit. Rev. Biochem.* **6,** 103–164
10. Geeves, M. A. (1991) *Biochem. J.* **274,** 1–14
11. Nascimento, A. A. C., Cheney, R. E., Tauhata, S. B. F., Larson, R. E., and Mooseker, M. S. (1996) *J. Biol. Chem.* **271,** 17561–17569
12. Johnson, K. A., and Taylor, E. W. (1978) *Biochemistry* **17,** 3432–3442
13. Cremo, C. R., and Geeves, M. A. (1998) *Biochemistry* **37,** 1969–1978
14. Kurzawa, S. E., and Geeves, M. A. (1996) *J. Muscle Res. Cell Motil.* **17,** 669–676
15. Collins, K., Sellers, J. R., and Matsudaira, P. (1990) *J. Cell Biol.* **110,** 1137–1147
16. Stevens, R. C., and Davis, T. N. (1998) *J. Cell Biol.* **142,** 711–722
17. Brockerhoff, S. E., Stevens, R. C., and Davis, T. N. (1994) *J. Cell Biol.* **124,** 315–323
18. Evans, L. L., Lee, A. J., Bridgman, P. C., and Mooseker, M. S. (1998) *J. Cell Sci.* **111,** 2055–2066
19. Jontes, J. D., Milligan, R. A., Pollard, T. D., and Ostap, E. M. (1997) *Proc. Natl. Acad. Sci. U. S. A.* **94,** 14332–14337
20. Woodward, S. K., Eccleston, J. F., and Geeves, M. A. (1991) *Biochemistry* **30,** 422–430
21. Geeves, M. A., and Conibear, D. A. (1995) *Biophys. J.* **68,** (suppl.) 194–201
22. Ma, Y.-Z., and Taylor, E. W. (1997) *J. Biol. Chem.* **272,** 717–723
23. Ma, Y.-Z., and Taylor, E. W. (1997) *J. Biol. Chem.* **272,** 724–730
24. Pechatnikova, E., and Taylor, E. W. (1997) *J. Biol. Chem.* **272,** 30735–30740
25. Hackney, D. D. (1995) *Nature* **377,** 448–450
26. Jiang, W., and Hackney, D. D. (1997) *J. Biol. Chem.* **272,** 5616–5621
27. Block, S. M., Goldstein, L. S., and Schnapp, B. J. (1990) *Nature* **348,** 348–352
28. Schnitzer, M. J., and Block, S. M. (1997) *Nature* **388,** 386–390
29. Ritchie, M. D., Geeves, M. A., Woodward, S. K., and Manstein, D. J. (1993) *Proc. Natl. Acad. Sci. U. S. A.* **90,** 8619–8623